J Biol Inorg Chem (2001) 6:367–377
DOI 10.1007/s007750100211

ORIGINAL ARTICLE

Leroy Cronin · Simon P. Foxon · Paul J. Lusby
Paul H. Walton

Syntheses and structures of M(L)(X)BPh4 complexes {M=Co(II), Zn(II); L=cis-1,3,5-tris[3-(2-furyl)prop-2-enylideneamino]cyclohexane, X=OAc, NO3}: structural models of the active site of carbonic anhydrase

Received: 23 November 2000 / Accepted: 9 January 2001 / Published online: 2 March 2001

Abstract The metal coordination geometries in the structures of the zinc(II) and cobalt(II) complexes of the ligand cis-1,3,5-tris[3-(2-furyl)prop-2-enylideneamino]cyclohexane (fr-protach) and with the anions nitrate and acetate are structural models for the active site of carbonic anhydrase. The acetate structures show a striking structural correlation with the metal coordination environments in the known bicarbonate forms of the enzyme. Such structures provide a basis for understanding the marked effect of different metal substitution on the catalytic rate of the enzyme.

Keywords Carbonic anhydrase · Triaminocyclohexane · Biomimicry · Zinc · Cobalt

Introduction

Human carbonic anhydrase II (HCA II) is one of the most efficient of known metal-containing enzymes, catalysing at near diffusion-limited rates (kcat/KM=3×108 dm3 mol–1 s–1) the hydration of carbon dioxide to bicarbonate and a proton [1, 2]. The enzyme and its isozymes have been investigated extensively; there are over 120 single-crystal X-ray diffraction structure studies that have been performed on the native enzyme, its mutants, isozymes and various metal-substituted forms [3][1]. These structural studies, coupled with theoretical and kinetic studies, have allowed many of the enzyme's mechanistic details to be elucidated ([2, 4] and references therein). Small-molecule model complexes have also played an important role in elucidating the mechanism. In particular, studies on monomeric Zn-hydroxide complexes have helped in establishing the role of zinc-bound hydroxide in CO2 hydration [5]. Overall, these studies show that the active site consists of a zinc(II) ion coordinated by three histidine residues at the bottom of a deep cavity, which is partly hydrophobic and partly hydrophilic in character. A water molecule coordinated to the zinc ion has a lowered pKa (ca. 7) such that it is deprotonated at physiological pH. The resulting hydroxide ion is a potent nucleophile, which attacks CO2 to give a coordinated bicarbonate anion. Expulsion from the active site of the bicarbonate ion, with concomitant coordination of a water molecule to zinc(II), completes the catalytic cycle.

The cobalt(II)-substituted form of HCA II exhibits roughly half the activity of the native enzyme, with all other metal-substituted forms showing little or no activity [6]. Such a strong dependence on metal substitution is not surprising in a biomolecular context, but is intriguing from a mechanistic point of view. The strong dependence suggests that the coordination properties of the metal ion, particularly for bicarbonate (stable coordination number and geometries, ligand exchange rates, etc.), are critical in determining the activity of the enzyme.

Of late, our work has concentrated on preparing and characterizing small-molecule model complexes of HCA II [7]. These models aim to help in understanding the enzyme's detailed mechanism of action, with an emphasis on understanding the differences in activities of the various metal-substituted forms of HCA II and as to the nature of the metal-bicarbonate intermediate.

Using a small-molecule model approach to help establish the mechanistic details of HCA II is hampered by the surprising lack of structurally characterized small-molecule bicarbonate complexes. A search

[1] The Research Collaboratory for Structural Bioinformatics, Protein Databank (RCSB PDB) can be located at the following www address: http://www.rcsb.org/pdb/

[1] The Research Collaboratory for Structural Bioinformatics, Protein Databank (RCSB PDB) can be located at the following www address: http://www.rcsb.org/pdb/

of the Cambridge Structural Database shows that there is a total of 13 metal-bicarbonate structures, with no known structures of bicarbonate coordinated to zinc(II) or cobalt(II) and only two cobalt(III) structures[2]. The most recent structures were published by van Eldik and co-workers [10], who determined the structures of two Cu(II)-bicarbonate complexes, with each exhibiting a different coordination mode of bicarbonate. The overall lack of bicarbonate complexes presumably reflects the inherent instability of the complexes with respect to decarboxylation and/or carbonate formation ([20] and references therein). To bypass the problem of inherent metal-bicarbonate instability, Looney and Parkin [21] have prepared small-molecule model complexes of HCA II which use nitrate as an isoelectronic mimic of bicarbonate. These studies of metal-nitrate complexes have helped in suggesting possible reasons for variations in the catalytic activity of metal-substituted versions of CA (see later). The models are valuable in providing sound chemical precedents for the binding of small oxo anions to biomimetic metal centres. However, there are some important differences between the model system and the enzyme, not least of which are the electronic differences between nitrate and bicarbonate, and "secondary interactions" (such as hydrogen bonds) which occur between the active site and the substrate, but which are not mimicked in the models.

In this paper we report a similar approach to mimicking the active site of HCA II, using acetate and nitrate as mimics of the bicarbonate ligand in zinc(II) and cobalt(II) complexes. The results show that caution must be exercised in interpreting the resultant small-molecule structures in terms of the catalytic activity of the enzyme [22]. However, the results also demonstrate that a clear difference exists in the coordination properties of zinc(II) and cobalt(II) towards oxo anions, which can, in turn, be correlated with enzyme activity.

In our previous studies we have used a ligand system based on cis-1,3,5-tris(propenylideneamino)cyclohexane derivatives (protach ligand system) to model the immediate face-capping tris-histidine metal coordination sphere seen in HCA II. Ligands based on tach have found increasing use in bioinorganic model complexes [23, 24, 25, 26]. The main attraction of these complexes [23, 26] is that they attempt to model not only the immediate metal coordination sphere of the metal in the enzyme, but also some features of the rest of the active site. In the study reported in this paper we have used the ligand cis-1,3,5-tris[3-(2-furyl)prop-2-enylideneamino]cyclohexane (L) [27] to prepare model complexes of HCA II. The general structure of the resulting complexes with L is shown in Fig. 1. L coordinates in an N3 face-capping geometry around the metal upon complexation, mimicking the N3 face-capping tris-histidine coordination geometry of the metal ion in HCA II. The furylpropenylidene "arms" surround the metal ion's remaining coordination site(s) with a rigid hydrophobic cavity. The cavity is an important feature of our ligand design since it provides a hydrophobic environment which – coupled with the overall +2 charge on the metal-ligand complex – models to some extent the electronic environment of the active site within the enzyme. The cavity also hinders dimerization of the complexes; hence we can study anion binding to a single metal ion, removing the potential for the anion to act as a bridging ligand. We have also performed our studies in a coordinating solvent, methanol, which acts as a mimic of water in the metal coordination sphere.

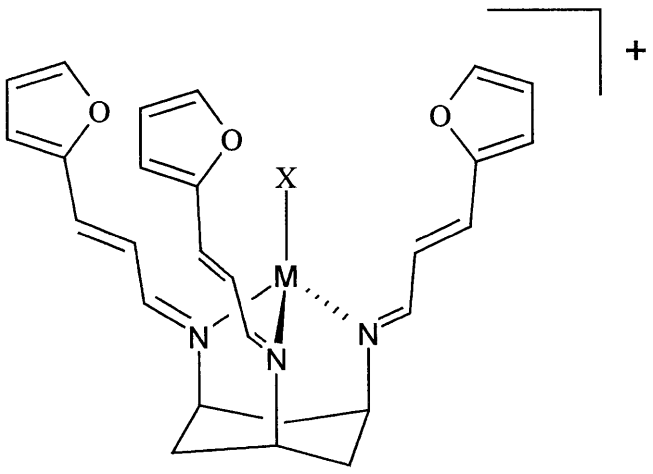

Fig. 1 cis-1,3,5-Tris[3-(2-furyl)prop-2-enylideneamino]cyclohexane-metal complexes [M=cobalt(II), zinc(II); X=NO3, MeCO2]

Materials and methods

Gases were supplied by BOC and were of commercial grade, being used without further purification. Solvents for synthesis (AR grade) were supplied by Fisons and were also used without further purification (unless stated). Deuterated solvents were obtained from Goss Scientific. All other reagents were supplied by Aldrich or Lancaster Chemicals and used without further purification (unless stated). Syntheses were carried out using Schlenk line techniques under nitrogen or argon. Melting points were determined using an Electrothermal 1100 microprocessor-controlled apparatus. FT-NMR spectra were acquired on JEOL FX90Q, JEOL EX270, Bruker MSL300 or Bruker AMX500 spectrometers. Referencing was achieved using the residual solvent protons in the solvent. IR spectra were acquired using a Mattson Sirius Research Series FTIR spectrometer as KBr pressed pellets (pressed under 7.0 tonnes pressure). Mass spectra were acquired on a Fisons Instruments Autospec using a 0–650 °C temperature range. X-ray diffraction data were collected on a Rigaku AFC6S four-circle diffractometer, with graphite monochromated Mo-Ka radiation; see Table 1 for details. Crystallographic data (without structure factors) for the structures reported in this paper have been deposited with the

[2] Stuctures of known metal-bicarbonate complexes: [8, 9, 10, 11, 12, 13, 14, 15, 16, 17, 18, 19]

Table 1 Single-crystal X-ray crystallographic data for complexes I–IV

	I	II	III	IV
Chemical formula	C53H55BN4O8Zn	C53H55BCoN4O8	C55H54BCl4N3O5Zn	C55H58BCoN3O7
Formula weight	952.19	945.75	1054.99	942.78
Crystal system	Orthorhombic	Orthorhombic	Triclinic	Orthorhombic
Space group	Pbca	Pbca	$P\bar{1}$	Pbca
μ (Mo Ka) (mm–1)	0.557	0.400	0.670	0.393
R1a (I)>2s(I)	0.0693	0.0681	0.0665	0.0946
wR2b (all data)	0.2113	0.2290	0.2057	0.3318
a (Å)	19.507(4)	19.403(9)	13.374(10)	19.277(17)
b (Å)	32.957(15)	32.755(12)	18.147(9)	33.583(14)
c (Å)	15.299(4)	15.729(5)	12.811(6)	15.652(5)
a (°)	90	90	108.91(4)	90
b (°)	90	90	102.56(5)	90
g (°)	90	90	71.09(5)	90
V (Å3)	9836(6)	9996(7)	2761(3)	10133(10)
T (K)	293(2)	293(2)	293(2)	293(2)
Z	8	8	2	8
Independent reflections	6496	6522	5125	6613

aR1=å||Fo|–|Fc||/å|Fo|
bwR2={å[w(Fo2–Fc2)2]/å[w(Fo2)2]}1/2

Cambridge Crystallographic Data Centre as supplementary publication nos. CDCC 151599–151602. Copies of the data can be obtained free of charge from the CDCC (12 Union Road, Cambridge CB2 1EZ, UK; tel.: +44-1223-336408; fax: +44-1223-336003; e-mail: deposit@cdcc.cam.ac.uk; www: http://ccdc.cam.ac.uk).

cis-1,3,5-Triaminocyclohexane (tach) [28]

cis-1,3,5-Cyclohexanetricarboxylic acid (22.50 g, 118.0 mmol) was stirred in benzene (500 cm3) and triethylamine (49.3 cm3, 353 mmol) was added, followed by the addition of diphenylphosphoryl azide (93.3 g, 353 mmol). The mixture was stirred for 0.5 h at ambient temperature and then refluxed for 0.5 h, causing complete dissolution. Benzyl alcohol (40.7 g, 393 mmol) was added and the solution was refluxed for 18 h, during which time a precipitate formed. After cooling to ambient temperature the solution was filtered and washed with cold benzene (200 cm3) and dried under vacuum to give the tribenzyl carbamate as a white powder (42.0 g, 76.9 mmol; 67%). Deprotection of the tribenzyl carbamate was achieved by addition of a 33% w/v hydrogen bromide in acetic acid solution (100 cm3) and stirring for 3.5 h, followed by addition of ethanol (200 cm3) and stirring for a further 1 h to give a white precipitate which was isolated by filtration. The residue was washed with ethanol (500 cm3) and diethyl ether (500 cm3) to give the crude triaminocyclohexane.3HBr as a white powder (25.9 g, 48.7 mmol; 88% from the carbamate).

Tach can be further purified using the following procedure. An aqueous solution (5 cm3) of tach.3HBr (2.00 g, 5.38 mmol) was applied to a basic ion-exchange column (DOWEX ion exchange resin, 20–50 mesh) and the amine eluted in water (ca. 250 cm3). Reduction in vacuo of the eluent gave a colourless oil, which was then dissolved in methanol (20 cm3). The methanol was removed under reduced pressure on a Schlenk line. The residue was sublimed in vacuo (10–2 mbar, 70 °C) on to a cold finger cooled at –78 °C. The product was isolated as a white crystalline solid (0.65 g, 5.0 mmol; 97%); m.p. 59–60 °C. 1H NMR (CD3OD, 500 MHz): d4.95 (s, H2O), 2.74 (tt, 3H, 3JHH=11.5 Hz, 3JHH=3.8 Hz, -CR2H), 2.04 [dt, 3H, 2JHH=11.5 Hz, 3JHH=3.8 Hz, -CH(Heq)-], 0.95 [dt, 3H, 3JHH=11.5 Hz, 2JHH=11.5 Hz, -CH(Hax)-]. IR/cm–1: 3332(m), 3258(m), 3166(m), 3925(m), 2926(m), 2853(m), 2758(m), 1571(s), 1473(m), 1457(m), 1386(m), 1349(m), 1274(w), 1172(w), 1148(w), 1050(w), 1005(m), 976(m), 901(w), 855(w), 821(w), 617(w). MS CI: +m/z=130 (MH+). Elemental analysis for C6H15N3.2/3H2O, actual (expected) %: C 50.8 (51.0), H 11.25 (11.65), N 29.85 (29.80).

cis-1,3,5-Tris[3-(2-furyl)prop-2-enylideneamino]cyclohexane (L)

cis-1,3,5-Triaminocyclohexane.3HBr (1.56 g, 4.19 mmol) and sodium hydroxide (0.503 g, 12.6 mmol) were dissolved in water (10 cm3) and added to a solution of 3-(2-furyl)acrolein (1.54 g, 12.6 mmol, previously recrystallized from water) in diethyl ether (25 cm3). The solution was stirred at room temperature for 5 h, giving a precipitate. The precipitate was isolated by filtration and dried in air to give the product as a cream-coloured powder (1.42 g, 3.22 mmol; 77%); m.p. 147°C (dec). 1H NMR (CD3OD, 270 MHz): d8.16 (d, 3H, 3JHH=9.2 Hz, -N=CH-), 7.66 (d, 3H, 3JHH=1.7 Hz, O-CH), 7.01 (d, 3H, 3JHH=16.0 Hz, -N=CHCH=CH-), 6.75 (dd, 3H, 3JHH=16.0 Hz, 3JHH=9.2 Hz, N=CHCH=), 6.68 (d, 3H, 3JHH=3.4 Hz, -CCH-), 6.56 (dd, 3H, 3JHH=3.4, 3JHH=1.7, -CH(CH)CH-), 4.93 (s, H2O), 3.52 (m, 3H, -CR2H-), 1.85 (m, 6H, >CH2). IR/cm–1 (KBr pressed pellet): 3660–3320(s), 3117(w), 3068(w), 2928(m), 2902(w), 2856(m), 1633(s), 1622(s), 1552(w), 1479(m), 1461(m), 1382(m), 1339(w), 1292(w), 1260(m), 1203(w), 1150(m), 1116(w), 1074(w), 1026(m), 1012(m), 983(m), 925(m), 884(m), 861(w), 816(w), 803(w), 743(m), 734(m), 664(w), 595(m), 564(m). MS FAB+(4-nitrobenzyl alcohol matrix): m/z=442 (MH+). Analysis calculated for L.1/2H2O, C27H28N3O3.5, actual (expected) %: C 72.0 (72.0), H 6.00 (6.25), N 9.25 (9.35).

{cis-1,3,5-Tris[3-(2-furyl)prop-2-enylidene)amino]-k3-N,N¢,N¢¢-cyclohexane}nitratozinc(II) tetraphenylborate (complex I)

A solution of zinc(II) nitrate hydrate (0.034 g, 0.113 mmol) in ethanol (4 cm3) was added to a solution of L (0.050 g, 0.113 mmol) in ethanol (2 cm3). A solution of NaBPh4 (0.039 g, 0.114 mmol) in ethanol (2 cm3) was added dropwise with stirring. A precipitate formed immediately, which was isolated by filtration and then dried in vacuo to give the product as a pale-yellow powder (0.068 g, 0.0766 mmol; 68%); m.p. 220–222 °C (dec). IR/cm–1 (KBr pressed pellet): 3600–3300(w), 3237(w), 3121(w), 3052(m), 2982(w), 2921(w), 1942(w), 1889(w), 1824(w), 1763(w), 1670(m), 1627(s), 1607(s), 1580(m,sh), 1559(w,sh), 1514(w), 1467(m), 1424(m,sh), 1384(s), 1270(m,b), 1214(w), 1172(m), 1120(m), 1072(w), 1018(m), 996(w), 949(w), 928(m), 884(m), 840(w), 815(w), 746(m), 734(m), 705(m), 612(m),

590(m). MS FAB+(4-nitrobenzyl alcohol matrix) m/z=567(M–BPh4–). Analysis calculated for I, C51H47 BN4O6Zn, actual (expected) %: C 69.0 (69.0), H 5.35 (5.30), N 6.00 (6.30).

{cis-1,3,5-Tris[3-(2-furyl)prop-2-enylidene)amino]-k3-N,N¢,N¢¢-cyclohexane}nitratocobalt(II) tetraphenylborate (complex II)

A solution of L (0.050 g, 0.113 mmol) in ethanol (2 cm3) was added to a solution of cobalt(II) nitrate hexahydrate (0.033 g, 0.113 mmol) in ethanol (2 cm3), giving a colour change from pale red to deep red. A solution of NaBPh4 (0.039 g, 0.114 mmol) in ethanol (3 cm3) was added with stirring, giving an instant pink precipitate. The precipitate was isolated by filtration and then dried in vacuo, giving the product as a pink powder (0.084 g, 0.091 mmol; 81%); m.p. 200–202 °C (dec). IR/cm–1 (KBr pressed pellet): 3523(m,sh), 3600–3300(w,br), 3054(m), 2922(w), 1626(s), 1605(s), 1580(m), 1504(w), 1471(m), 1416(w), 1385(s), 1265(m), 1174(m), 1124(w), 1074(w), 1018(m), 994(w), 958(w), 928(w), 884(m), 736(m), 708(m), 613(w), 591(w), 511(w). MS FAB+(4-nitrobenzyl alcohol matrix) m/z=562 (M–BPh4–). Analysis calculated for II, C51H51BCoN4O8, actual (expected) %: C 67.0 (66.7), H 5.95 (5.60), N 5.90 (6.10).

{cis-1,3,5-{Tris[3-(2-furyl)prop-2-enylidene)amino-k3-N,N¢,N¢¢]} cyclohexane}acetatozinc(II) tetraphenylborate (complex III)

A solution of zinc(II) acetate hydrate (0.025 g, 0.113 mmol) in methanol (2 cm3) was added to a solution of L (0.050 g, 0.113 mmol) in methanol (3 cm3). A solution of NaBPh4 (0.039 g, 0.114 mmol) in methanol (2 cm3) was added dropwise with stirring. A precipitate formed which was isolated by filtration and then dried in vacuo to give the product as a cream-coloured powder (0.077 g, 0.087 mmol; 77%); m.p. 220–222 °C (dec). IR/cm–1 (KBr pressed pellet): 3600–3300(s), 3053(s), 2992(m), 2924(m), 1630(s), 1611(s), 1582(m), 1563(m), 1471(s), 1424(m), 1388(s), 1332(m), 1267(m), 1216(m), 1172(s), 1121(s), 1075(m), 1017(s), 1000(m), 930(m), 884(m), 748(s), 733(s), 707(s), 615(m), 593(m). MS FAB+(4-nitrobenzyl alcohol matrix) m/z=564 (M–BPh4–). Analysis calculated for III.1/2H2O, C53H51BN3O5.5Zn, actual (expected) %: C 71.2 (71.2), H 5.70 (5.75), N 4.55 (4.70).

{cis-1,3,5-{Tris[3-(2-furyl)prop-2-enylidene)amino-k3-N,N¢,N¢¢]} cyclohexane}acetatocobalt(II) tetraphenylborate (complex IV)

A solution of L (0.050 g, 0.113 mmol) in ethanol (2 cm3) was added to a solution of cobalt(II) acetate tetrahydrate (0.038 g, 0.130 mmol) in ethanol (2 cm3), giving a colour change from pale red to blood red. A solution of NaBPh4 (0.039 g, 0.114 mmol) in ethanol (3 cm3) was added, giving an instant precipitate. The precipitate was isolated by filtration and then dried in vacuo to give the product as a purple-coloured powder (0.075 g, 0.085 mmol; 75%); m.p. 209–210 °C (dec). IR/cm–1 (KBr pressed pellet): 3600–3300(w,br), 3117(w), 3055(m), 2998(w), 2919(w), 1947(w), 1885(w), 1821(w), 1752(w), 1627(s), 1609(s), 1579(s), 1473(s), 1425(m), 1388(m), 1461(w), 1266(m), 1215(m), 1172(s), 1119(s), 1074(m), 1018(s), 991(m), 948(w), 929(m), 884(m), 846(w), 814(w), 752(s), 735(s), 705(s), 611(m), 582(m), 570(w), 519(w). MS FAB+(4-nitrobenzyl alcohol matrix) m/z=559 (M–BPh4–). Analysis calculated for IV, C53H50 BCoN3O5, actual (expected) %: C 72.8 (72.4), H 5.75 (5.75), N 4.85 (4.80).

Results and discussion

The synthesis of cis-1,3,5-triaminocyclohexane (tach) followed the procedure published by Bowen et al. [28]. It was found that the triamine could be further purified by sublimation to give the product as a slightly hygroscopic, white crystalline solid. The tach.3HBr salt could be readily reacted with 2-furylacrolein to give the ligand L in reasonable yield. Synthesis of the metal complexes was achieved by adding solutions of the appropriate metal salt to L, followed by metathesis of one of the anions with BPh4– (Scheme 1). The BPh4– counter anion was found not to coordinate to the metal centre (see below). Yields for the complexes ranged from 68 to 81%.

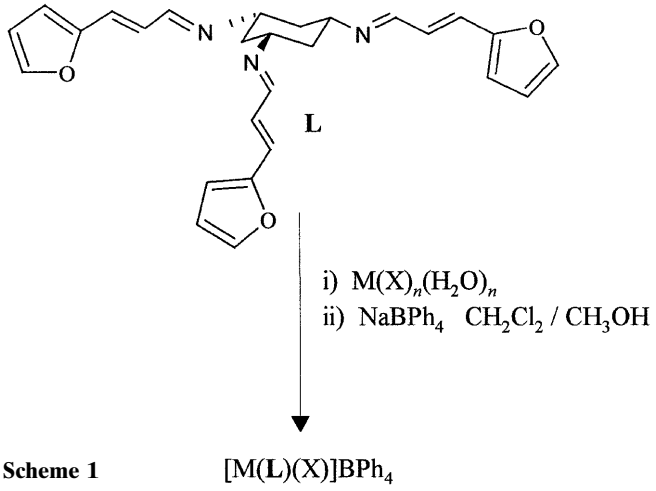

Scheme 1 [M(**L**)(X)]BPh_4

The complexes could be recrystallized by allowing a MeOH or mixed CH2Cl2/MeOH solution of the complex to evaporate slowly. In all cases, crystals suitable for single-crystal X-ray diffraction were obtained (Table 1). All complexes have the same general structure, with L coordinating in the expected N3 face-capping fashion (Figs. 2, 3, 4, 5) with the furylpropenylidene "arms" forming a rigid cavity around the metal's remaining coordination sites. In each case a single acetate or a single nitrate is coordinated to the metal ion, where the anion is encapsulated within the cavity of the complex. In some cases a methanol molecule is also coordinated to the metal ion. The BPh4– counter anion is "outside" the cavity and does not affect the immediate metal coordination sphere.

The main differences in the structures lie in their metal coordination geometries. The nitrate complexes of the zinc(II) and cobalt(II) structures (I and II) show the same basic coordination geometry with a bidentate nitrate ligand and a methanol molecule coordinating in the sixth coordination site (Figs. 2 and 3). However, comparison of the acetate structures (III and IV) shows marked differences in the zinc(II) and cobalt(II) coordination geometries (Figs. 4 and 5).

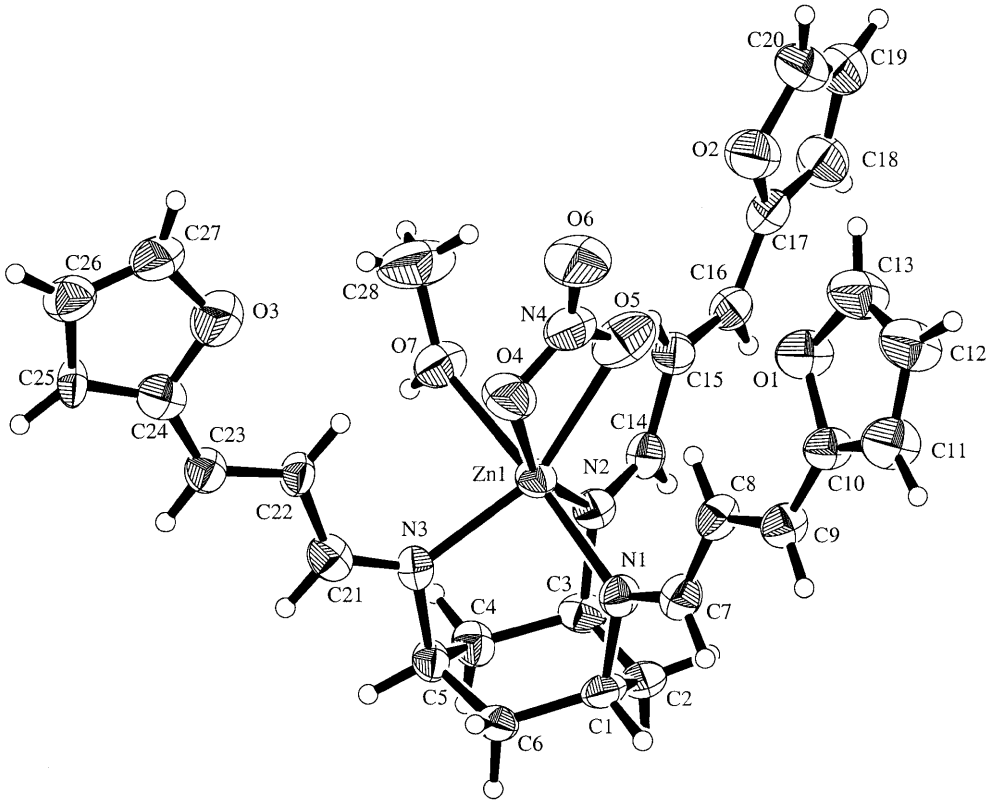

Fig. 2 ORTEP [33] representation (30%) ellipsoids) of [Zn(L)(NO3)(MeOH)]BPh4 (BPh4 anion omitted for clarity)

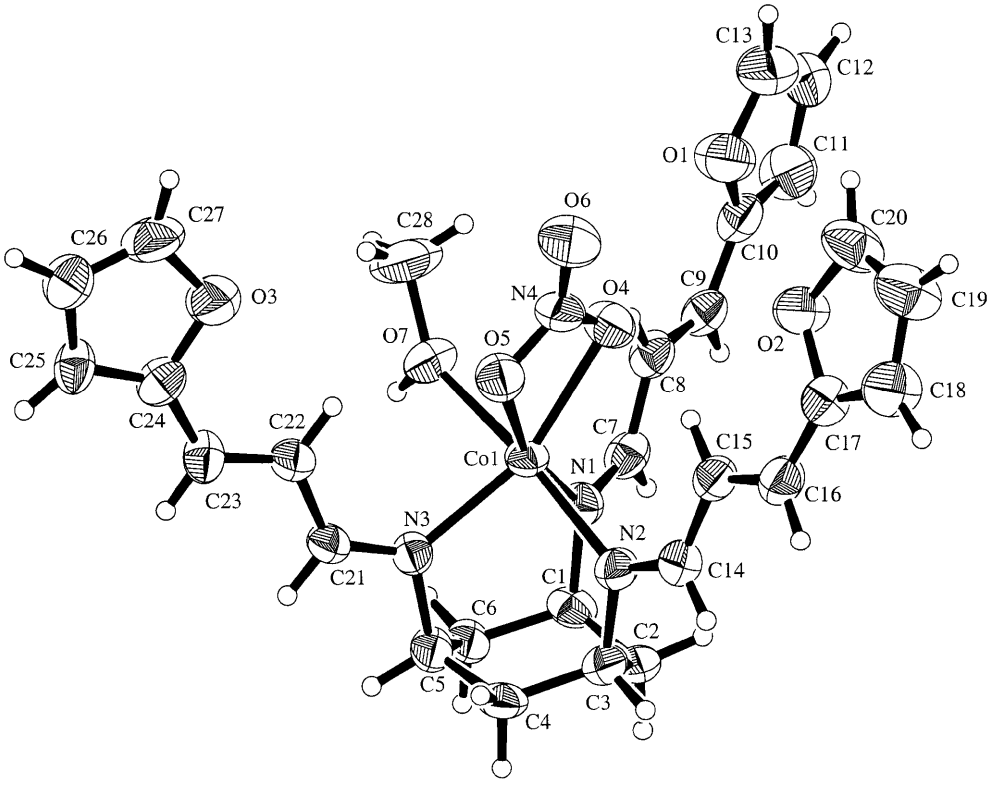

Fig. 3 ORTEP [33] representation (30%) ellipsoids) of [Co(L)(NO3)(MeOH)]BPh4 (BPh4 anion omitted for clarity)

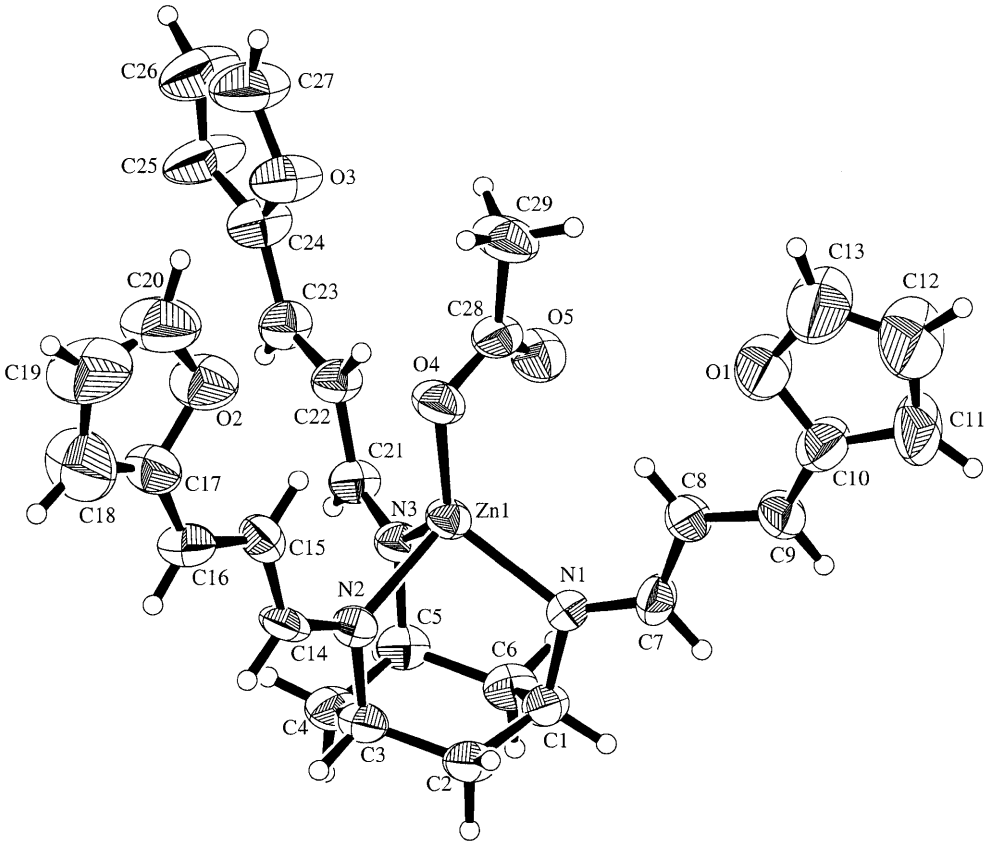

Fig. 4 ORTEP [33] representation (30%) ellipsoids) of [Zn(L)(OAc)]BPh4 (BPh4 anion omitted for clarity)

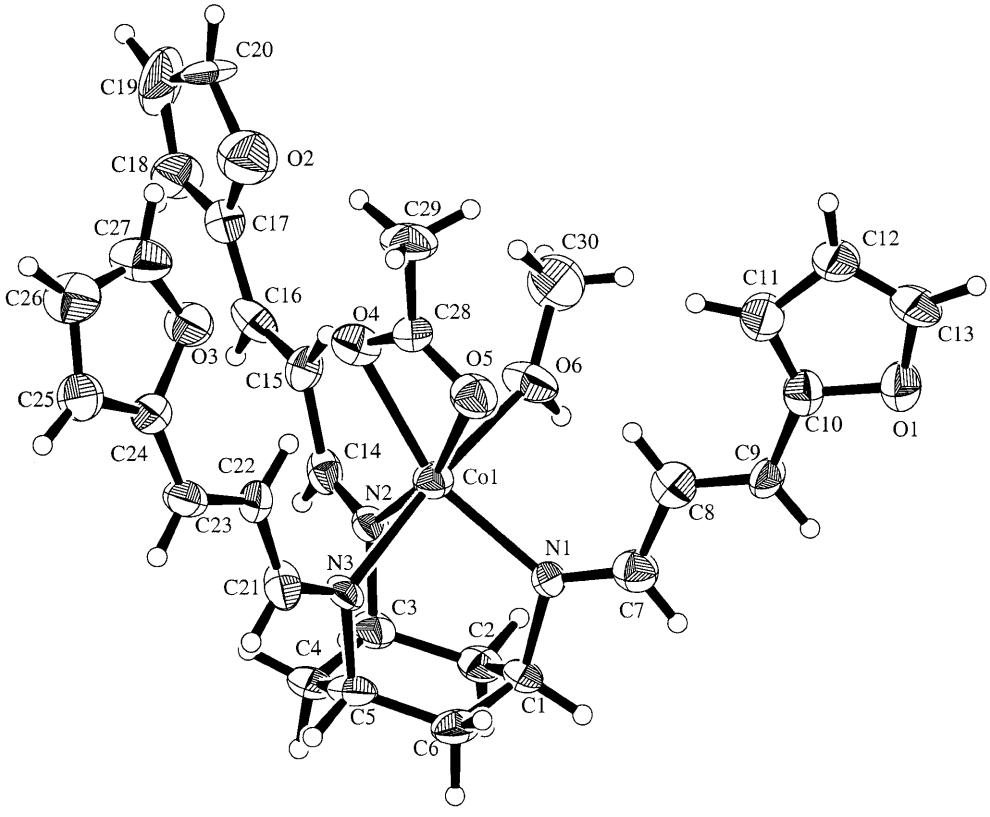

Fig. 5 ORTEP [33] representation (30%) ellipsoids) of [Co(L)(OAc)(MeOH)]BPh4 (BPh4 anion omitted for clarity)

Table 2 Metal coordination sphere parameters (distances in Å, angles in °) for complexes I–IV

Parameter		Parameter	
Complex I			
Zn(1)-O(4)	2.162(8)	Zn(1)-N(1)	2.114(6)
Zn(1)-O(5)	2.342(8)	Zn(1)-N(2)	2.048(7)
Zn(1)-O(7)	2.278(6)	Zn(1)-N(3)	2.068(7)
O(4)-Zn(1)-O(5)	55.1(3)	N(3)-Zn(1)-O(4)	101.8(3)
O(4)-Zn(1)-O(7)	85.6(2)	Zn(1)-N(1)-C(7)	128.8(6)
O(5)-Zn(1)-O(7)	82.7(2)	Zn(1)-N(2)-C(14)	130.3(6)
N(1)-Zn(1)-O(4)	101.6(3)	Zn(1)–N(3)–C(21)	130.4(6)
N(2)-Zn(1)-O(4)	157.8(3)		
Complex II			
Co(1)-O(4)	2.221(6)	Co(1)-N(1)	2.091(7)
Co(1)-O(5)	2.154(6)	Co(1)-N(2)	2.174(6)
Co(1)-O(7)	2.180(5)	Co(1)-N(3)	2.083(6)
O(4)-Co(1)-O(5)	59.0(2)	N(3)-Co(1)-O(4)	157.9(3)
O(4)-Co(1)-O(7)	84.9(2)	Co(1)-N(1)-C(7)	127.9(6)
O(5)-Co(1)-O(7)	88.9(2)	Co(1)-N(2)-C(14)	129.3(6)
N(1)-Co(1)-O(4)	104.7(3)	Co(1)-N(3)-C(21)	129.0(5)
N(2)-Co(1)-O(4)	102.3(2)		
Complex III			
Zn(1)-O(4)	1.930(6)	O(4)-Zn(1)-O(5)	55.9(3)
Zn(1)-O(5)	2.584(7)	N(1)-Zn(1)-O(4)	125.1(3)
		N(2)-Zn(1)-O(4)	109.9(3)
		N(3)-Zn(1)-O(4)	128.9(3)
Zn(1)-N(1)	2.038(7)	Zn(1)-N(1)-C(7)	130.6(6)
Zn(1)-N(2)	2.059(8)	Zn(1)-N(2)-C(14)	131.7(6)
Zn(1)-N(3)	2.042(7)	Zn(1)-N(3)-C(21)	129.1(6)
Complex IV			
Co(1)-O(4)	2.189(9)	O(4)-Co(1)-O(5)	59.8(4)
Co(1)-O(5)	2.156(9)	O(4)-Co(1)-O(6)	84.5(3)
Co(1)-O(6)	2.241(9)	O(5)-Co(1)-O(6)	87.9(3)
		N(1)-Co(1)-O(4)	158.4(4)
		N(2)-Co(1)-O(4)	103.7(4)
Co(1)-N(1)	2.102(10)	N(3)-Co(1)-O(4)	103.9(4)
Co(1)-N(2)	2.097(10)	Co(1)-N(1)-C(7)	129.4(9)
Co(1)-N(3)	2.174(9)	Co(1)-N(2)-C(14)	126.9(9)
		Co(1)-N(3)-C(21)	128.8(9)

The metal coordination geometries and their relevance to HCA II are described below.

Nitrate complexes

For the nitrate complexes there is little difference in the metrical parameters of the metal coordination spheres (Table 2). Comparison of these complexes cannot therefore be used to explain the differences in reactivity seen in the native and cobalt(II)-substituted enzyme. Significantly, in the model complexes the role of solvent is apparent: a methanol molecule coordinates to give a six-coordinate metal ion with a bidentate nitrate anion. A similar coordination mode for bicarbonate and water is seen in the structure of cobalt-substituted HCA II [29], whereas the coordination mode of bicarbonate to zinc(II) in HCA II (Thr200®His200 mutant) is monodentate with no water coordination [30][3]. The tendency of nitrate in our systems to coordinate in a bidentate fashion to the metal centres is not surprising. Moreover, in the complexes presented in this paper, bidentate nitrate coordination is facilitated by coordination of a solvent molecule to give the metal ion in a near-octahedral coordination geometry. Therefore, in a coordinating solvent it is likely that for all of our metal complexes the coordination mode of nitrate will be bidentate. Thus, the use of nitrate as an isoelectronic mimic of bicarbonate is limited when used in coordinating solvents. Nevertheless, it is perhaps important to note that coordination numbers greater than 4 can be formed at biomimetic zinc(II) centres and such coordination numbers are possible when considering possible detailed mechanisms of action of HCA II.

Acetate complexes

In terms of mimicking bicarbonate, it appears as if the acetate anion may be a better model than nitrate. One of the reasons for the difference between acetate and nitrate is that, upon coordination to a metal, both bicarbonate and acetate anions possess major res-

[3] There is a further known structure of a HCA II with coordinated bicarbonate [31]. We have not used this structure for comparison purposes since it contains a key mutation of residue Thr199. We believe that Thr199 is a critical determinant of the bicarbonate binding mode

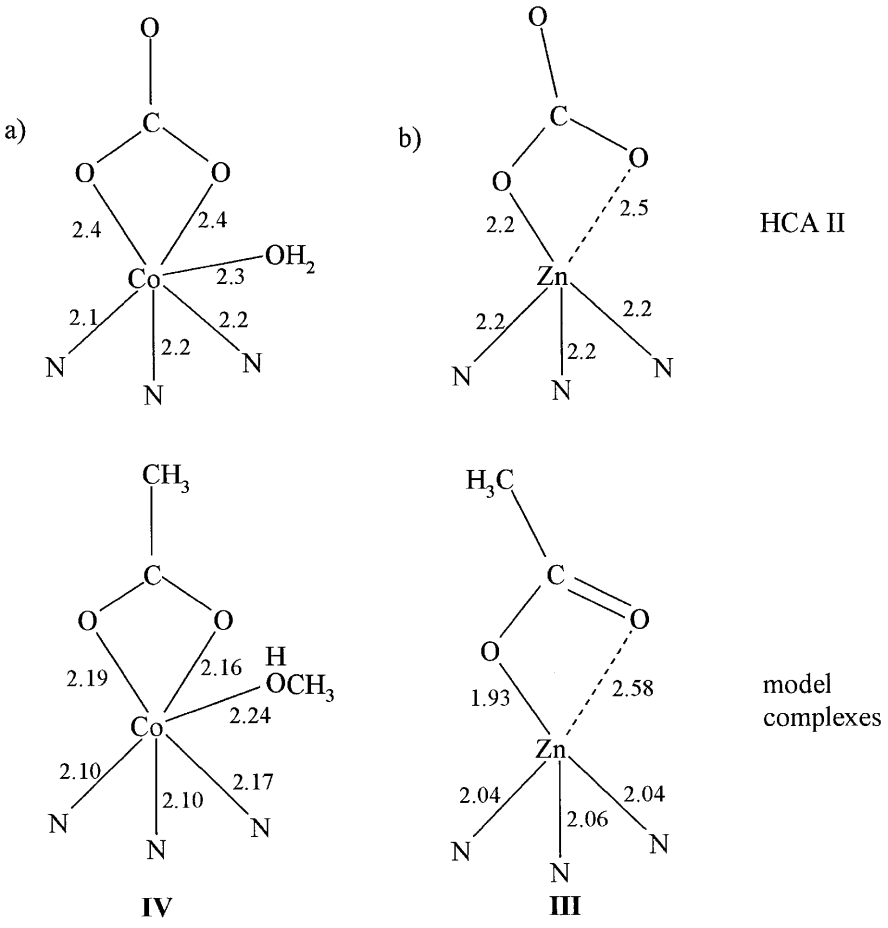

Fig. 6 Comparison of coordination geometries of the metal in [M(OAc)(L)]+ complexes to those in a cobalt-substituted HCA II and b HCA II (Thr200®His200)

onance forms which concentrate negative charge on a single coordinating oxygen atom [22]. Thus, on charge separation grounds, the tendency to coordinate in a bidentate mode is less for acetate and bicarbonate than for nitrate.

The increased tendency of acetate to give monodentate coordination is observed in the structures of the acetate complexes of cobalt(II) and zinc(II) with L. The main difference between the two structures lies in the coordination mode of the acetate ion. In the zinc(II) complex the acetate is nearly monodentate [Zn-O(4)=1.930(6) Å, Zn...O(5)=2.584(7) Å] (Fig. 4); in the cobalt(II) complex the acetate is clearly bidentate [Co-O(4)=2.189(9) Å, Co-O(5)=2.156(9) Å] with a methanol molecule also coordinating to the cobalt(II) (Fig. 5). It is significant that the monodentate coordination of acetate to zinc(II) occurs even in the presence of potentially coordinating solvent molecules. The difference in the coordination modes of acetate in the two complexes highlights the coordination geometry preferences of zinc(II) and cobalt(II).

Comparison of the two structures presented here with structures of the bicarbonate forms of HCA II (Thr200®His200) and cobalt(II)-substituted HCA II shows a striking structural correlation between the binding mode of acetate in our structures and the binding mode of bicarbonate seen in the enzymes. The key metrical values of the metal coordination sphere in the enzymes and in our model complexes are similar (see Fig. 6). The coordination mode of the bicarbonate in the structure of HCA II (Thr200® His200) exhibits the same near-monodentate coordination as the acetate in the model complex, with a weak second interaction [Zn...O(1)=2.5 Å] between a bicarbonate oxygen and the zinc(II) ion. In contrast, the structure of the bicarbonate form of cobalt(II)-substituted HCA II shows a bidentate bicarbonate mirroring the binding mode of acetate seen in our cobalt(II)

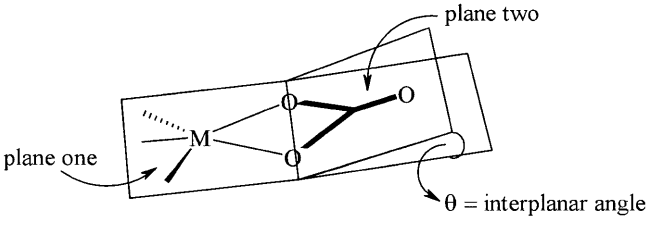

Fig. 7 Imaginary planes defined by (plane one) bicarbonate and (plane two) the metal-oxygen-oxygen plane of a bicarbonate chelate; q=interplanar angle

Table 3 List of q values (see Fig. 7) for structurally determined small-molecule metal-bicarbonate complexes

Complexa	HCO3– binding mode	Interplanar angle q (°)	Ref
[Pd(II)(dppe)(OCO2H)2]	Monodentate	10.88 and 12.31	[8]
[Pt(II)(Ph)(OCO2H)(PEt3)2]	Monodentate	11.31	[9]
[Cu(II)(phen)2(OCO2H)]ClO4	Monodentate	2.88	[10]
[W(CO)5(OCO2H)][PPN]	Monodentate	0.16	[11]
[Pd(II)(Me)(PEt3)2(OCO2H)]	Monodentate	No data available	[12]
Rh(CO)(PPh3)2(OCO2H)]	Monodentate	No data available	[13]
[Co(III)(tepa)(O2COH)](ClO4)2	Bidentate	4.14	[14]
[Ru(II)(R)(CO)(O2COH)(PPh3)2]	Bidentate	3.29	[15]
[Cd(II)(Me4Cyclam)(O2COH)]ClO4	Bidentate	2.76	[16]
[Co(III)(acac)(py)2(O2COH)]	Bidentate	2.46	[17]
[Cu(II)(STTP)(OCO2H)]	Bidentate	2.26	[18]
[Rh(III)(H)2(O2COH)(iPr3P)2]	Bidentate	0.2	[19]
[Cu(II)(phen)2(O2COH]ClO4	Bidentate	0.0	[10]

adppe=1,2-bis(diphenylphosphino)ethane; phen=1,10-phenanthroline; PPN=bis(triphenylphosphino)iminium; tepa=tris[2-(2-pyridyl) ethyl]amine; R=1,2-bis(dimethoxycarbonyl)ethenyl; Me4Cyclam=1,4,8,11-tetramethyl-1,4,8,11-tetraazacyclotetradecane; acac=2,4-pentanedione; py=2-aminopyridine; STTP=21-thiatetra-p-tolylporphyrin

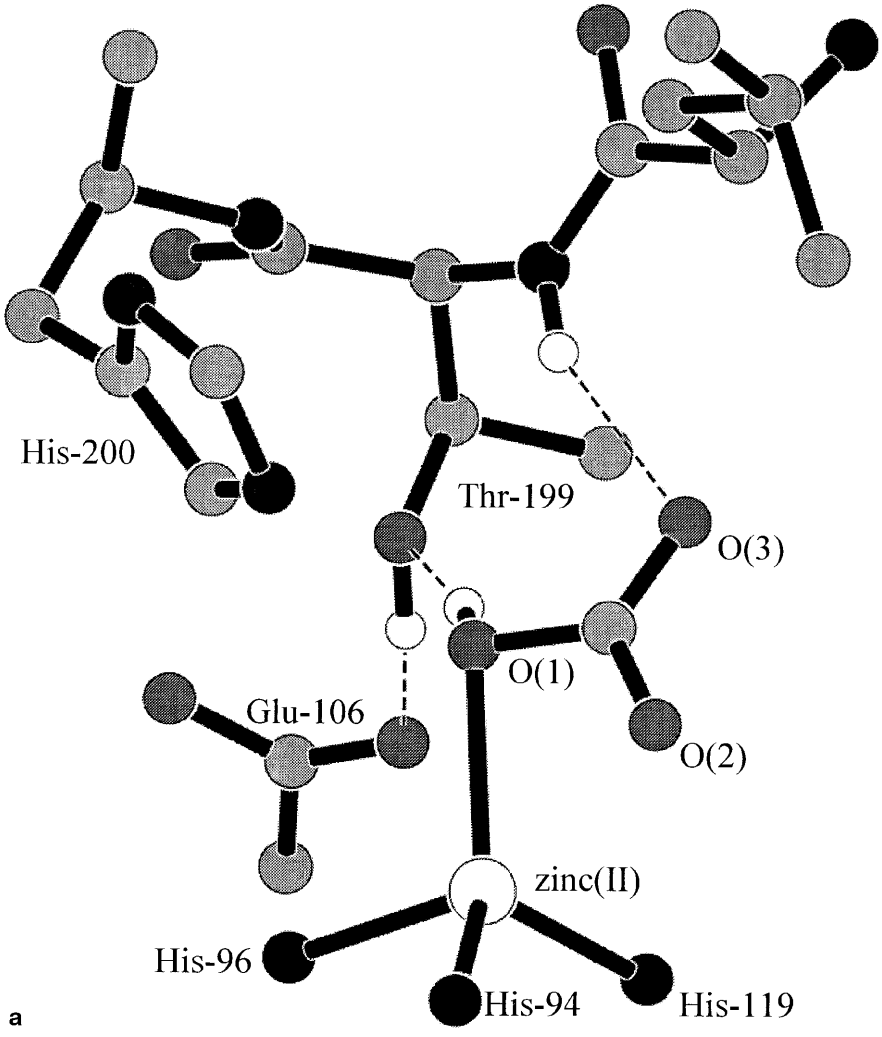

Fig. 8 Hydrogen-bonding interaction between coordinated bicarbonate and active site in a Thr200®His200 mutant HCA II [30] and b cobalt-substituted HCA II [29]. Hydrogen atoms from amino acid side chains have been omitted for clarity. The HCO3– hydrogen is placed on the coordinating oxygen, consistent with a proposed H-bond to Og-Thr199

model complex. Moreover, the coordination of a methanol molecule in the model complex mimics the coordination of water to cobalt(II) which is observed in the structure of the enzyme. The similarities also extend to the orientation of the acetate/bicarbonate best-fit plane with respect to the three Zn-N bonds, and to the small angle between the Zn-O vector and the near C3 axis of the metal ion in the tris-histidine coordination.

There are some important differences between the model complexes and the enzyme. The metal-ion to ligand distances are generally shorter in the model complexes compared to those in the enzyme. Also, in the structures of both cobalt(II) and zinc(II) forms of HCA II, the best fit plane of the bicarbonate ion is skewed by about 34° from the plane defined by the metal ion and the two coordinating oxygen atoms of the bicarbonate; in other words the bicarbonate is "bent back" in the enzyme (Fig. 7). In our model complexes the analogous interplanar angle is near 0°. Also, in known metal-bicarbonate complexes [8, 9, 10, 11, 12, 13, 14, 15, 16, 17, 18, 19] the interplanar angle is small (most<5°, all<13°; see Table 3).

Some of the discrepancies between the model complexes and the enzyme can be attributed to the relatively large error in bond distances for the enzyme structures [~0.16 Å in the zinc(II) structure and ~0.18 Å in the cobalt(II) structure]. However, the differences are almost certainly due to the presence of certain hydrogen bonds to bicarbonate in the enzyme which are not present in the model complexes. In particular, hydrogen-bond interactions formed between a nearby amino acid (Thr199) and the bicarbonate anion are probably the main reason for bicarbonate adopting the "bent back" coordination mode shown in Fig. 8. Many authors have speculated on the role of Thr199 in the catalytic mechanism; from our studies it appears as if Thr199 has a role in restricting the coordination mode of the bicarbonate anion, such that it must adopt a "bent back" coordination geometry.

Conclusions

The structures presented in this paper show that nitrate and acetate are not necessarily good mimics for the binding of bicarbonate to metal ions in HCA II. The main reasons lie in the differences in the coordinating properties between the model anions and bicarbonate. Also, the model complexes do not accurately mimic the environment of the enzyme's active

Fig. 8 b

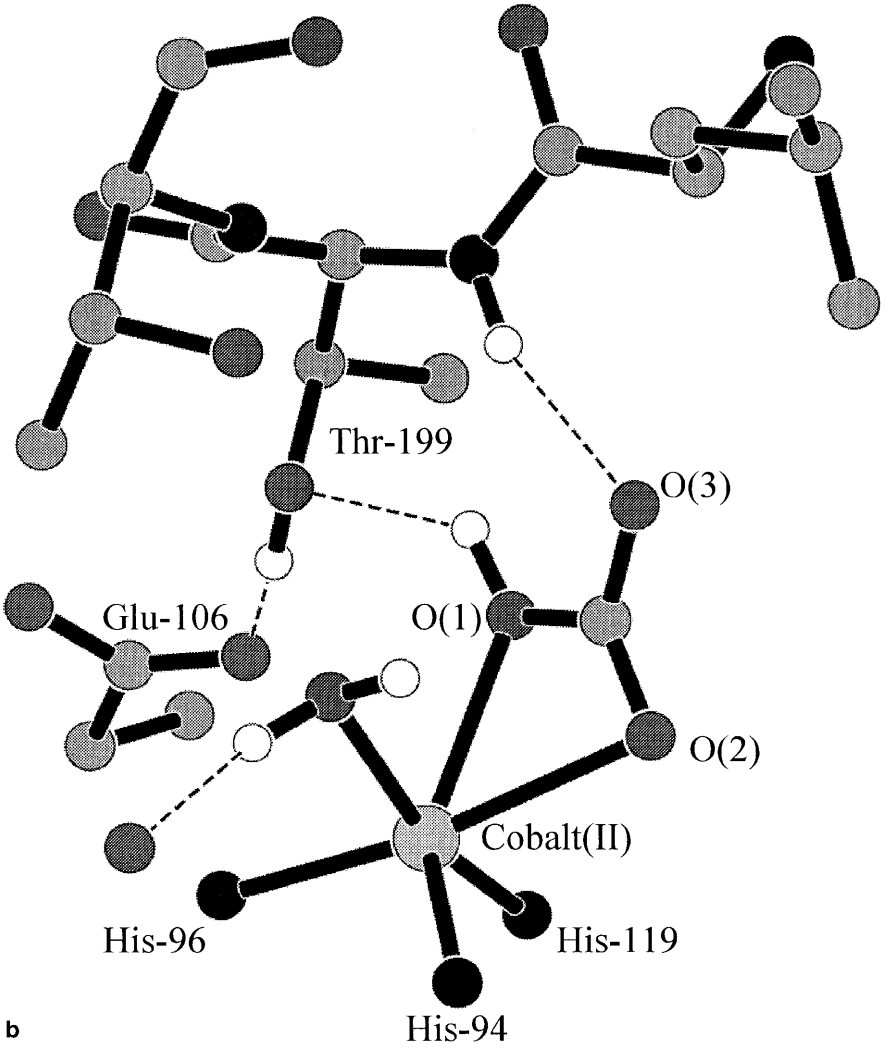

site, especially the presence of hydrogen bonds between the active site and the substrate. Accordingly, caution must be exercised in drawing analogies between the structures of our metal complexes and those observed in the enzyme.

Nevertheless, the analogies between the metrical parameters of the metal coordination geometries in the acetate complexes and those seen for bicarbonate in the enzyme structures suggest that the energetic demands of the metal coordination sphere are indeed significant factors in determining the mode of oxo-anion binding in both the model complexes and the enzyme; a similar conclusion was reached by Looney and Parkin [21]. The importance of solvent coordination is especially clear. In the zinc(II) complex, simultaneous coordination by solvent and bicarbonate/acetate appears to be energetically less favourable than the single coordination by bicarbonate/acetate, whereas in the cobalt(II) case the opposite appears to be true. Indeed, in our system, four-coordinate cobalt(II) model complexes with acetate or nitrate could not be prepared in the presence of methanol molecules. In HCA II the reduced activity of the cobalt(II)-substituted form of HCA II compared to the wild-type enzyme may well be related to the greater tendency of cobalt(II) to form complexes with coordination numbers higher than four in the presence of coordinating solvents.

The model complexes, as well as demonstrating the tendency of zinc(II) complexes to remain four coordinate, also indicate that in HCA II the possible coordination modes of bicarbonate are severely restricted by Thr199. The acetate model complexes and known small-molecule bicarbonate-metal complexes suggest that bicarbonate would coordinate to the metal ions in a "planar" fashion (i.e. that the metal-oxygen-oxygen plane, as defined earlier, is near co-planar with the best fit plane of the bicarbonate). In the structures of HCA II (Thr200®His200) and cobalt(II)-substituted HCA II, hydrogen bonds between the coordinated bicarbonate and Thr199 cause the bicarbonate to be "bent back" from the coordination mode expected from small-molecule studies. Such a restriction of bicarbonate binding to the metal ion correlates with the remarkably weak inhibition of HCA II by bicarbonate (at pH 7, Ki=150 mmol dm–3 [32]) and is also consistent with a highly efficient catalytic mechanism for CO2 hydration.

Acknowledgements L.C. and S.P.F. acknowledge the EPSRC for the provision of maintenance grants.

References

1. Bertini I, Luchinat C (1994) In: Bertini I, Gray HB, Lippard SJ, Valentine JS (eds) Bioinorganic chemistry. University Science Books, Mill Valley, Calif., pp 37–107
2. Silverman DN, Lindskog S (1988) Acc Chem Res 21:30–36
3. Berman HM, Westbrook J, Feng Z, Gilliland G, Bhat TN, Weissig H, Shindyalov IN, Bourne PE (2000) Nucleic Acids Res 28:235–242
4. Toba S, Colombo G, Merz KM Jr (1999) J Am Chem Soc 121:2290–2302
5. Kimura E, Shiota T, Koike T, Shiro M, Kodama M (1990) J Am Chem Soc 112:5805–5811
6. Eriksson EA, Jones TA, Liljas A (1986) In: Bertini I, Luchinat C, Maret W, Zeppezauer M (eds) Zinc enzymes. Birkhäuser, Boston, pp 28–37
7. Boxwell CJ, Walton PH (1999) Chem Commun 1647–1648
8. Ganguly S, Mague JT, Roundhill DM (1992) Inorg Chem 31:3831–3835
9. Ito M, Ebihara M, Kawamura T (1994) Inorg Chim Acta 218:199–202
10. Mao Z-W, Liehr G, van Eldik R (2000) J Am Chem Soc 122:4839–4840
11. Darensbourg DJ, Meckfessel Jones ML, Reibenspies JH (1996) Inorg Chem 35:4406–4413
12. Crutchley RJ, Powell J, Faggiani R, Lock CJL (1977) Inorg Chim Acta 24:L15–L16
13. Hossain SF, Nicholas KM, Teas CL, Davis RE (1981) J Chem Soc Chem Commun 268–269
14. Baxter KE, Hanton LR, Simpson J, Vincent BR, Blackman AG (1995) Inorg Chem 35:2795–2796
15. Romero A, Santos A, Vegas A (1988) Organometallics 7:1988–1993
16. Ito H, Ito T (1985) Acta Crystallogr Sect C 41:1598–1602
17. Döring M, Meinert M, Uhlig E, Dahlenburg L, Fawzi R (1991) Z Anorg Allg Chem 598:71–82
18. Latos-GraŸyñski L, Lisowski J, Olmstead MM, Balch AL (1987) J Am Chem Soc 109:4428–4429
19. Yoshida T, Thorn DL, Okano T, Ibers JA, Otsuka S (1979) J Am Chem Soc 101:4212–4221
20. Nakata K, Uddin MK, Ogawa K, Ichikawa K (1997) Chem Lett 991–992
21. Looney A, Parkin G (1994) Inorg Chem 33:1234–1237
22. Pavan Kumar PN, Marynick DS (1993) Inorg Chem 32:1857–1859
23. Greener B, Moore MH, Walton PH (1996) Chem Commun 27–28
24. Itoh T, Hisada H, Sumiya T, Honsons M, Usui Y, Fujii Y (1997) Chem Commun 677–678
25. Brand U, Vahrenkamp H (1992) Inorg Chim Acta 198–200:663–669
26. Greener B, Foxon SP, Walton PH (2000) New J Chem 24:269–273
27. Greener B, Cronin L, Wilson GD, Walton PH (1996) J Chem Soc Dalton Trans 3337–3339
28. Bowen T, Planalp RP, Brechbiel MW (1996) Bioorg Med Chem Lett 6:807–810
29. Håkansson K, Wehnert AJ (1992) J Mol Biol 228:1212–1218
30. Xue Y, Vidgren J, Svensson LA, Liljas A, Jonsson B-H, Lindskog S (1993) Proteins Struct Funct Genet 15:80–87
31. Xue Y, Liljas A, Jonsson B-H, Lindskog S (1993) Proteins Struct Funct Genet 17:93–106
32. Krebs JF, Rana F, Dluhy RA, Fierke CA (1993) Biochemistry 32:4496–4505
33. Johnson CK (1976) ORTEP II, a FORTRAN thermal-ellipsoid plot program. Oak Ridge National Laboratory, Oak Ridge, Tenn., report ORNL-5138